MATEC Web of Conferences **45**, 02002 (2016)
DOI: 10.1051/matecconf/20164502002
© Owned by the authors, published by EDP Sciences, 2016

An Improved VI-CFAR Detector Based on GOS

Likai Zhao, Sen Li and Guangzhao Hu

School of Information and Electronics, Beijing Institute of Technology, Beijing 100081, P. R. China

Abstract. In combination with the advantages of CA-CFAR, GO-CFAR and SO-CFAR algorithm, the VI-CFAR has strong adaptability both in homogeneous and non-homogeneous environment. However, if the interfering targets are present in both the halves of the reference sliding windows, the use of the window with the smallest mean is affected by them and therefore results in a performance degradation. In order to overcome the shortcoming, an improved VI-CFAR detector based on GOS (IVI-CFAR) is proposed in this paper. We introduce the IVI-CFAR detector and make performance simulation and analysis in homogenous and non-homogenous environment. In the homogeneous environment, the IVI-CFAR detector has some CFAR loss relative to the CA-CFAR detector. In the clutter edge environment, the IVI-CFAR detector keeps the good performance of the VI-CFAR detector. In multiple interfering targets environment, the IVI-CFAR detector performs robustly, which is similar to the OS-CFAR detector. In addition, the IVI-CFAR detector shortens the sample sorting time of the OS-CFARR detector.

1 Introduction

In radar and sonar signal detection, in order to get a constant false alarm (CFAR) performance, the actual average power of interfering background will be estimated by the reference cells near the test cell to adaptively set the detection threshold. For the different method of background power estimation, the method of CFAR is also different. Conventional CFAR detectors include average cell CFAR (CA–CFAR[1]) detector and order statistics CFAR (OS-CFAR[2]) detector. Under the homogeneous background, the CA-CFAR detector can get close to the optimal detection performance, but in the non-homogeneous environment, the detection performance of CA-CFAR seriously declines. When the actual number of the interfering targets is less than the predetermined number, the OS-CFAR detector has good detection performance, and in the homogeneous environment the CFAR loss can also be acceptable. However, in the clutter edge environment, the OS-CFAR detector has a high false alarm peak, then the false alarm control ability is poor. In order to overcome the disadvantages of the CFAR detectors, the VI-CFAR detector was proposed by Smith and Varshney [3, 4]. In this detector, the data in the reference sliding window is used to compute two statistics VI and MR. Based on these statistics, two tests are performed in order to select the algorithms (CA-CFAR, GO-CFAR [5] and SO-CFAR [6]) to be used for the estimation of the clutter power in the test cell [7]. So the detector combines the advantages of the CA-CFAR, GO-CFAR and SO-CFAR algorithms. Under the homogeneous background, the VI-CFAR detector has a small CFAR loss relative to the CA-CFAR detector. Under the non-homogeneous background, the VI-CFAR detector also has strong robustness. However, when the interfering targets appear in both the leading and lagging sliding window, the possibility of the VI-CFAR detector selecting the SO-CFAR algorithm increases, this will lead to the serious deterioration of the performance of the VI-CFAR detector. Based on the OS-CA CFAR algorithm [8, 9], an improved VI-CFAR (IVI-CFAR) detector is introduced .Through the Monte-Carlo simulation trials, this paper simulates the IVI-CFAR detectors detection and analyses the detection performance.

This paper is organized as follows. Section 2 introduces the principle of the VI-CFAR detector. In Section 3, an IVI-CFAR detector is proposed and the principle of the IVI-CFAR detector is introduced in detail. Simulation results and discussions are given in Section 4. And we make conclusions in Section 5.

2 The Principle VI-CFAR Detector

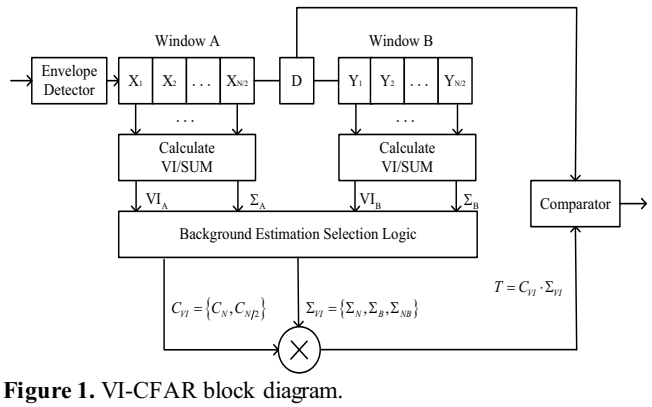

Figure 1. VI-CFAR block diagram.

This is an Open Access article distributed under the terms of the Creative Commons Attribution License 4.0, which permits unrestricted use distribution, and reproduction in any medium, provided the original work is properly cited.
Article available at http://www.matec-conferences.org or http://dx.doi.org/10.1051/matecconf/20164502002

Figure 1 is the block diagram of the VI-CFAR detector, where D is the test cell, the length of the leading reference sliding window A or the lagging reference sliding window B is N/2. Through VI and MR, the VI-CFAR detector adaptively selects the reference sliding window to estimate the background clutter power. Adaptive detection threshold T is equal to the product of the threshold factor C_{VI} and the background clutter power estimation. According to the comparison result of the test cell with the detection threshold T, the VI-CFAR detector judges whether the target exists or not. Adaptive decision criterion is: if D>T, the result is H_1 and the target exists in the test cell; if D≤T, the result is H_0, and the target does not exist in the test cell.

This article assumes that the signal is independent, identically distributed (IID), zero mean, Gaussian random process. Consequently, the envelope amplitude at the output of the square-law detector is an exponentially distributed random variable. The samples in the reference sliding window are independent of each other and of the sample in the test cell. When a target is present in the test cell, the use of guard cells (not shown in Figure 1) between the test cell and the reference sliding window prevents target energy from corrupting the reference sliding window.

The VI-CFAR detector utilizes the VI as well as the MR to select the subset of reference cells used for background clutter estimation. The test statistics are defined by formula (1) and (2) respectively. In order to reduce the computational, VI can be simplified as VI*, of which the defined formula is shown by formula (3). In formula (1)-(3), $\hat{\sigma}^2$ is the estimated population variance, and $\hat{\mu}$ is the estimated population mean. X_i is the samples of the leading or lagging half of the reference sliding window. $\overline{X}$ is the arithmetic mean of X_i in a half reference sliding window, and n equals N/2, N is the size of the whole reference sliding window.

$$VI = 1 + \frac{\hat{\sigma}^2}{\hat{\mu}^2} = 1 + \frac{1}{n-1} \cdot \sum_{i=1}^{n} \left(X_i - \overline{X} \right)^2 \Big/ \left(\overline{X} \right)^2 \tag{1}$$

$$MR = \overline{X}_A \Big/ \overline{X}_B = \sum_{i \in A} X_A \Big/ \sum_{i \in B} X_B \tag{2}$$

$$\begin{aligned} VI^* &= 1 + \frac{\hat{\sigma}^2}{\hat{\mu}^2} = 1 + \frac{1}{n} \cdot \sum_{1}^{n} \left(X_i - \overline{X} \right)^2 \Big/ \left(\overline{X} \right)^2 \\ &= n \cdot \sum_{i=1}^{n} \left(X_i \right)^2 \Big/ \left(\sum_{i=1}^{n} X_i \right)^2 \end{aligned} \tag{3}$$

By the following two hypothesis tests formula (4) and formula (5), the VI-CFAR detector determines whether the background is homogeneous or not, and adaptively selects the reference sliding window to adopt corresponding CFAR algorithm

$$\begin{cases} VI \le K_{VI} \Rightarrow \text{Homogeneous clutter background} \\ VI > K_{VI} \Rightarrow \text{Non-homogeneous clutter background} \end{cases} \tag{4}$$

$$\begin{cases} K_{MR}^{-1} \le MR \le K_{MR} & \Rightarrow \text{Same Mean} \\ MR > K_{MR} \text{ or } MR < K_{MR}^{-1} & \Rightarrow \text{Different Mean} \end{cases} \tag{5}$$

K_{VI} and K_{MR} are VI and MR decision thresholds respectively. The selections of them have relation to predetermined false-alarm probability and confidence levels. The corresponding error probability is shown in equation (6) and equation (7) respectively.

$$\alpha_0 = P\left(VI > K_{VI} \middle| \text{Homogeneous background} \right) \tag{6}$$

$$\beta_0 = 1 - P\left(K_{MR}^{-1} \le MR \le K_{MR} \middle| \text{Same Mean} \right) \tag{7}$$

By the above equations (6)-(7), the improvement of threshold K_{VI} and K_{MR} can reduce the error probability respectively. But at the same time, the judgment sensitivity of non-homogeneous background also can be reduced.

3 An Improved VI-CFAR Detector Based on GOS

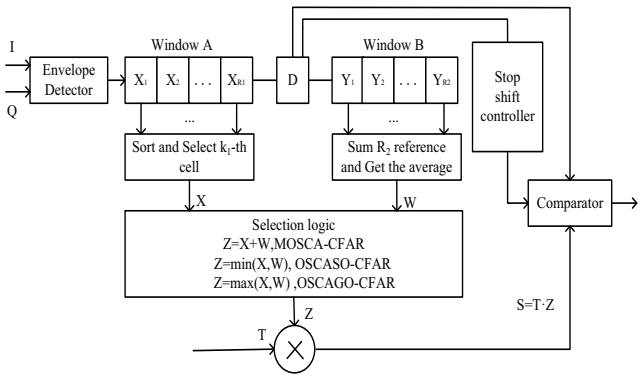

Figure 2. OS-CA CFAR block diagram.

According to the Figure 2, the OS-CA CFAR detector block diagram can be seen. The common characteristic of the OS-CA CFAR detector is: the leading reference sliding window makes local estimation in OS method, the lagging reference sliding window makes local estimate in CA method. At the same time, stop shift control logic constitutes the automatic screening technology with a reference cell shift register. When a target is declared in the test cell D, the lagging reference sliding window stops shift to eliminate the sample in the test cell.

According to the outcomes of the VI hypothesis test and MR hypothesis test, the IVI-CFAR detector adaptively chooses corresponding CFAR detection algorithm. When the clutter edge is present, the IVI-CFAR detector adopts the OSCAGO-CFAR and the order value k_1 of the OSCAGO-CFAR is set to a large value. When the interfering targets exist in the leading reference sliding window or the lagging reference sliding window, the IVI-CFAR detector also uses the OSCAGO-CFAR, but the order value k_2 of the OSCAGO-CFAR is set to a small value. When the interfering targets exist in both the halves of the reference sliding window, the IVI-CFAR detector adopts the OSCASO-CFAR.

The specific adaptive threshold production rules and the corresponding CFAR algorithm selections of the IVI-CFAR detector are shown in **Table 1**. C_N, C_{OSCAGO} and C_{OSCASO} are the threshold multiplier factors, which correspond to different CFAR method. Σ_{AB} , Σ_A and Σ_B are the sums of the whole and the half reference sliding respectively. $X_A(k_1)$, $X_A(k_2)$ and $X_A(k_3)$ are the

local estimation of the leading reference sliding window in OS method respectively. $X_B(k_2)$ is the local estimation of the lagging reference sliding window in OS method.

Table 1. IVI-CFAR Adaptive Threshold.

Leading Window Variable?	Lagging Window Variable?	Different mean?	Adaptive Threshold	CFAR Algorithm
No	No	No	$C_N \cdot \Sigma_{AB}$	CA
No	No	Yes	$C_{OSCAGO}(k_1) \cdot OSCAGO_{\max\left(X_A(k_1), \frac{1}{n}\Sigma_B\right)}(k_1)$	OSCAGO
Yes	No	-	$C_{OSCAGO}(k_2) \cdot OSCAGO_{\max\left(X_A(k_2), \frac{1}{n}\Sigma_B\right)}(k_2)$	OSCAGO
No	Yes	-	$C_{OSCAGO}(k_2) \cdot OSCAGO_{\max\left(X_B(k_2), \frac{1}{n}\Sigma_A\right)}(k_2)$	OSCAGO
Yes	Yes	-	$C_{OSCASO}(k_3) \cdot OSCASO_{\min\left(X_A(k_3), \frac{1}{n}\Sigma_B\right)}(k_3)$	OSCASO

Under the homogeneous background, the threshold multiplier factor C_N is determined based on CA-CFAR with N cells as shown in formula (8) [10]:

$$C_N = P_{fa}^{-1/N} - 1 \tag{8}$$

When the interfering targets are present in a single half of the reference sliding window or the clutter edge is around the test cell, the calculation of C_{OSCAGO} is based on OSCAGO-CFAR as shown in formula (9):

$$\begin{aligned} P_{fa}^{\text{OSCAGO}} = {} & \frac{R_1!\Gamma(R_1 - k + C_{OSCAGO} + 1)}{\Gamma(R_1 + C_{OSCAGO} + 1)} \\ & - \frac{1}{R_2}\sum_{i=0}^{R_2-1}\sum_{j=0}^{k-1}\binom{k-1}{j}(-1)^j \\ & \times \left(\frac{R_2}{R+1-k+j+C_{OSCAGO}}\right)^{i+1} \\ & + \sum_{i=k}^{R_1}\binom{R_1}{i}\sum_{j=0}^{i}\binom{i}{j}(-1)^i \\ & \times \left(\frac{R_2}{R-i+j+C_{OSCAGO}}\right)^{R_2} \end{aligned} \tag{9}$$

In the presence of interfering targets in both the halves of the reference sliding window, the value of C_{OSCAGO} is based on OSCASO-CFAR and obtained by formula (10):

$$\begin{aligned} P_{fa}^{\text{OSCASO}} = {} & \frac{1}{\left(1 + C_{OSCASO}/R_2\right)^{R_2}} + k\binom{R_1}{k}\frac{1}{R_2}\sum_{i=0}^{R_2-1}\sum_{j=0}^{k-1}\binom{k-1}{j}(-1)^j \\ & \times \left(\frac{R_2}{R+1-k+j+C_{OSCASO}}\right)^{i+1} \\ & - \sum_{i=k}^{R_1}\binom{R_1}{i}\sum_{j=0}^{i}\binom{i}{j}(-1)^i \\ & \times \left(\frac{R_2}{R-i+j+C_{OSCASO}}\right)^{R_2} \end{aligned} \tag{10}$$

4 Simulation results and discussions

To illustrate the detection performance of the IVI-CFAR detector in homogeneous and non-homogeneous environments characterized by the presence of interfering targets and the presence of clutter edge, we adopt 100000 Monte-Carlo simulation trials. The whole reference sliding window size N is 36, the P_{fa} is fixed to 10^{-4}, and the main target(in test cell) and interfering targets are both Swerlling Ⅱ. The confidence level of VI hypothesis test α_0 is fixed to 3.3×10^{-4}, the confidence level of MR hypothesis test β_0 is set as 0.08 and corresponding K_{VI} and K_{MR} are equal to 4.76 and 1.806 respectively[11].

4.1. Performance in Homogeneous Environment

Figure 3 shows the probability of detection (P_d) of the IVI-CFAR, CA-CFAR, GO-CFAR, SO-CFAR and VI-CFAR in the homogeneous environment. The symbol "OS(30)" denotes that the order value of the OS-CFAR is 30. The symbol "IVI(15,6,10)" denotes that the order value of the OSCAGO-CFAR is 15 in clutter edge environment and 6 when interfering targets exist in a

single half of the reference sliding window. In addition, the order value of the OSCASO-CFAR is 10 when the interfering targets are present in both halves of the reference sliding window. From Figure 3,we can see that the IVI-CFAR detector has a little CFAR loss relative to the CA-CFAR and outperforms the GO-CFAR and VI-CFAR detectors. When P_d=0.5, the CFAR loss of the IVI-CFAR relative to the CA-CFAR is about 0.1 dB. The CFAR loss for the VI-CFAR relative to the IVI-CFAR is about 0.15dB.

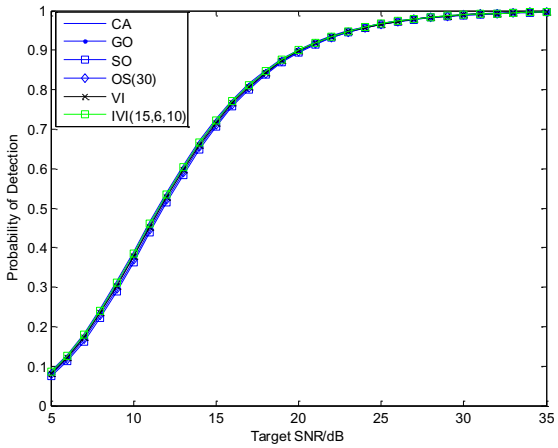

Figure 3. P_d comparison of the CFAR detectors in homogeneous environment.

4.2. Performance in Multi-target Environment

It is assumed that interfering-to-noise ratio (INR) is equal to the signal-to-noise ratio (SNR) in the multi-target environment in this paper[12]. In order to analyse the different effect of interfering targets location in the reference sliding window on the detection performance of the VI and IVI-CFAR, this paper analyses in two different conditions [12], i.e. the interfering targets only appear in the leading reference sliding window A and the interfering targets exist in the both halves of reference sliding window at the same time.

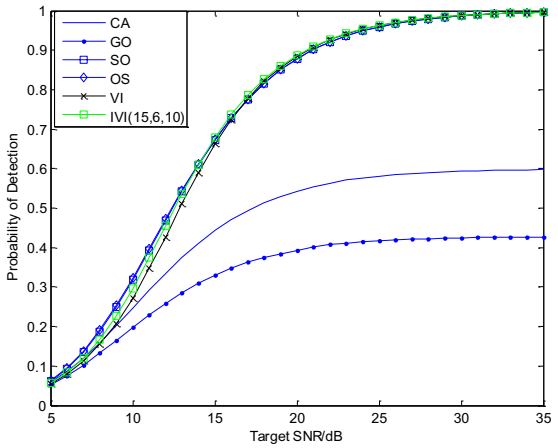

Figure 4. P_d comparison of the CFAR detectors when two interfering targets in window A.

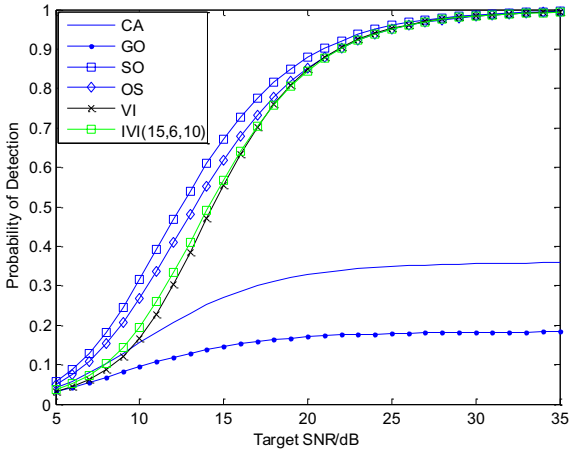

Figure 5. P_d comparison of the CFAR detectors when four interfering targets in window A.

Figure 4 and **Figure 5** show the P_d of the CA-CFAR, GO-CFAR, SO-CFAR, OS-CFAR, VI-CFAR and IVI-CFAR in the case of two interfering targets in the leading reference sliding window and four interfering targets in the lagging reference sliding window respectively. As can be seen, the IVI-CFAR exhibits a low CFAR loss relative to the SO-CFAR and outperforms the VI-CFAR and VI-CFAR. With the increase of the value of SNR, the P_d of IVI-CFAR and VI-CFAR approach that of OS-CFAR. In Figure 4,when P_d=0.5, the CFAR loss of the IVI-CFAR relative to the SO-CFAR is about 0.15 dB. The CFAR loss of the VI-CFAR relative to the IVI-CFAR is about 0.3dB.

Figure 6 shows the P_d of the CA-CFAR, GO-CFAR, SO-CFAR, OS-CFAR, VI-CFAR and IVI-CFAR in the case of two interfering targets in both the halves of the reference sliding window. It can be seen from Figure 6 that the thresholds of both the VI-CFAR and SO-CFAR are overestimated, so the detection performance degerade quickly while the OS-CFAR and IVI-CFAR perform well.

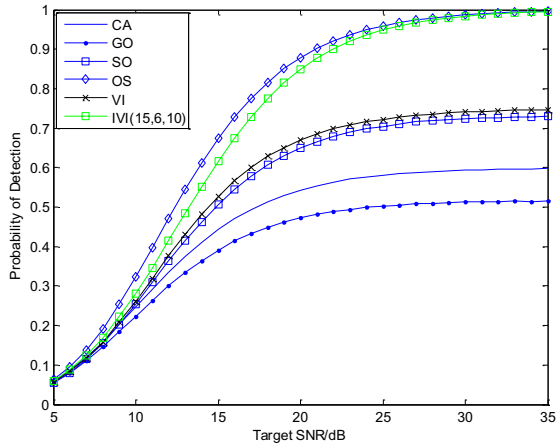

Figure 6. P_d comparison of the CFAR detectors when one interfering target in each half window.

4.3. Performance in Clutter Edge Environment

It is assumed that clutter envelope obeys Rayleigh distribution, and clutter-to-noise ratio is CNR. In Monte-Carle simulation trails, the clutter edge progressed from

left to right(window A to window B). The P_{fa} of the CA,GO,SO,OS,VI and IVI-CFAR in clutter edge environment is shown in **Figure 7** where the CNR is equal to 10dB. In this case, it can be seen that the false-alarm regulation properties of the IVI-CFAR and VI-CFAR are almost consistent. The false-alarm regulation properties of the CA-CFAR and OS-CFAR are poor relatively and that of SO-CFAR is the worst.

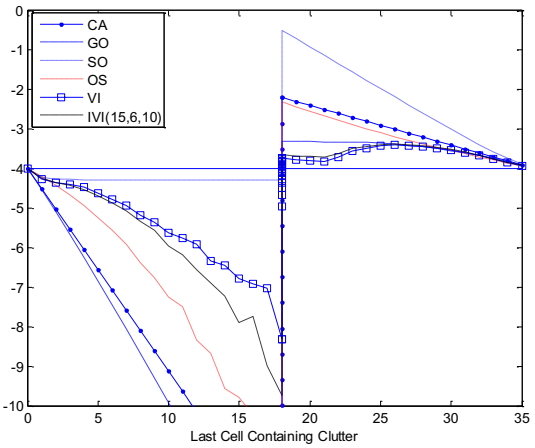

Figure 7. P_{FA} comparison of the CFAR detectors in clutter edge (CNR=10dB) environment

5 Conclusions

In this paper, we have presented an improved version of VI-CFAR, called IVI-CFAR detector and have analyzed the performance of the proposed IVI-CFAR detector in a homogeneous and non-homogeneous environments. In the homogeneous environment, the detection performance of the IVI-CFAR detector has some CFAR loss relative to the CA-CFAR detector and outperforms the GO-CFAR and VI-CFAR detectors. In the multiple targets situations, the IVI-CFAR detection is more robust than the VI-CFAR detector when the interfering targets are present in both the halves of the reference sliding window. In clutter edge environment, the performance of the IVI-CFAR detector is almost consistent with that of the VI-CFAR. In addition, the false-alarm regualtion property of the IVI-CFAR is even better than that of the GO-CFAR.

Acknowledgment

This research was supported in part by the National Natural Science Foundation of China under Grant No. 61421001, 61331021, 61172176 and 61490691

References

1. HM. Finn, RS.Johson, RCA Review.**29**, 50(1968)
2. H. Rohling, IEEE Transaction on AES, **19**,13 (1983)
3. ME.Smith,PK.Varshney.IEEEINTLRADAR,6 (1997)
4. ME.Smith,PK.Varshney. IEEE Transaction on AES,**36**,11 (2000)
5. V.G. Hansen, IEEEINTLRADAR,8 (1973)
6. G.V. Trunk., IEEE Transaction on AES,**14**,6 (1978)
7. K. Cheikh, F. Soltani, ICSIPA2011,4 (2011)
8. H. You, G. Jian, P. Yning, L. Dajin, CIC, 3 (1996)
9. Y. He, J. Guan, IEEE, 3 (1995)
10. K.Siddiq,IEEE, 4(2006)
11. A.Cong, Y.Xu, Q.Yao. IEEE, **9**,4(2011)
12. W.Hu, Y.Wang, S.Wang, IEEE, 4(2006)